Renyi and Tsallis statistics and their application to turbulence and vortex tangle

Toshihico Arimitsu (U of Tsukuba)
Naoko Arimitsu (Yokohama Nat'l U)

Introduction

Turbulence in a wind tunnel

(Experiment conducted by Mouri)

Introduction

In this talk…

- We introduce the method of multifractal analysis (MFA) which provides us with the expressions of the probability density functions (PDFs) in a unified compact analytical formula valid for various quantities in turbulence.
- The formula can explain, precisely, the experimentally observed PDFs both on log (showing their fat-tail part) and linear (showing their center part) scales.

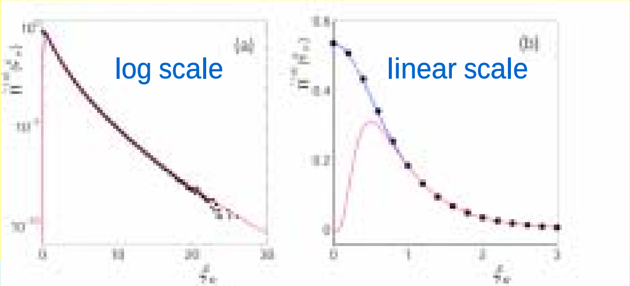

Introduction

In this talk…

- It will be shown, first, in the analyses of two beautiful experiments of normal fluid turbulence:
  - Bodenschatz et al. in the Lagrangian measurement of fluid particle accelerations.
  - Gotoh et al. in the DNS (Direct Numerical Simulation) with 1024^3 mesh size.
- Then, we proceed to analyze an experiment of superfluid turbulence to show MFA works also for this case, and to see if there appears some difference between classical and quantum turbulences:
  - Maurer & Tabeling in the observation of tangle.

Intermittency in a wind tunnel

A typical setup of the observation of fully developed turbulence behind a grid in a wind tunnel

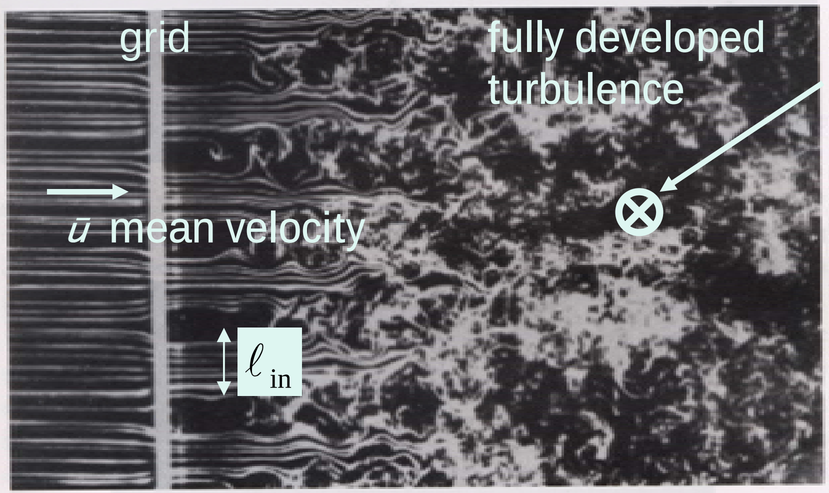

Fig. 1.11. Homogeneous turbulence behind a grid. Photograph T. Corke and H. Nagib. (from U.Frisch, *Turbulence* 1995)

Observe the wind velocities $u(t)$ by a x-array hot wire prove.

by Mouri (2004)
$R_\lambda = 249$,
$\bar{u} = 10$ [m/sec]
$\ell_{\text{in}} \approx 20$ [cm]

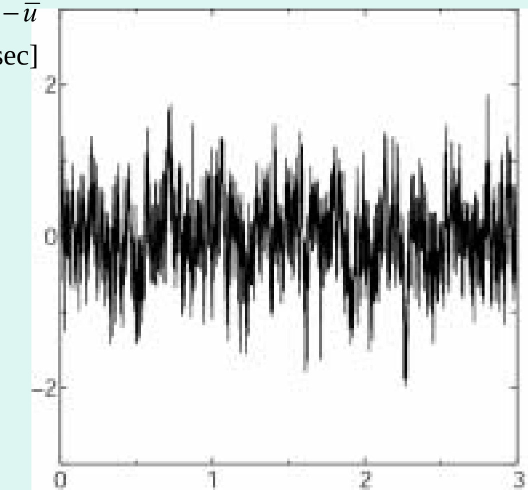

The observed time series of the longitudinal velocity component $u(t)$-$\bar{u}$ represents its chaotic changes in time.

Intermittency in a wind tunnel

The velocity differences $\delta u(t;\delta t) = u(t+\delta t) - u(t)$ for δt = 3.3x10^{-5} [sec] and δt = 1.3x10^{-2} [sec] are shown. The former represents intermittent character, whereas the latter looks like mere fluctuating behavior.

The velocity differences are scaled by their standard deviations:

$$\xi(t;\delta t) = \delta u(t;\delta t) \Big/ \sqrt{\langle \delta u(t;\delta t)^2 \rangle}$$

With the help of the Taylor frozen hypothesis, we can translate the time difference δt into the spatial distance δr by the relation, $\delta r = \bar{u}\,\delta t$.

Kolmogolov scale: η = 0.22 [mm].

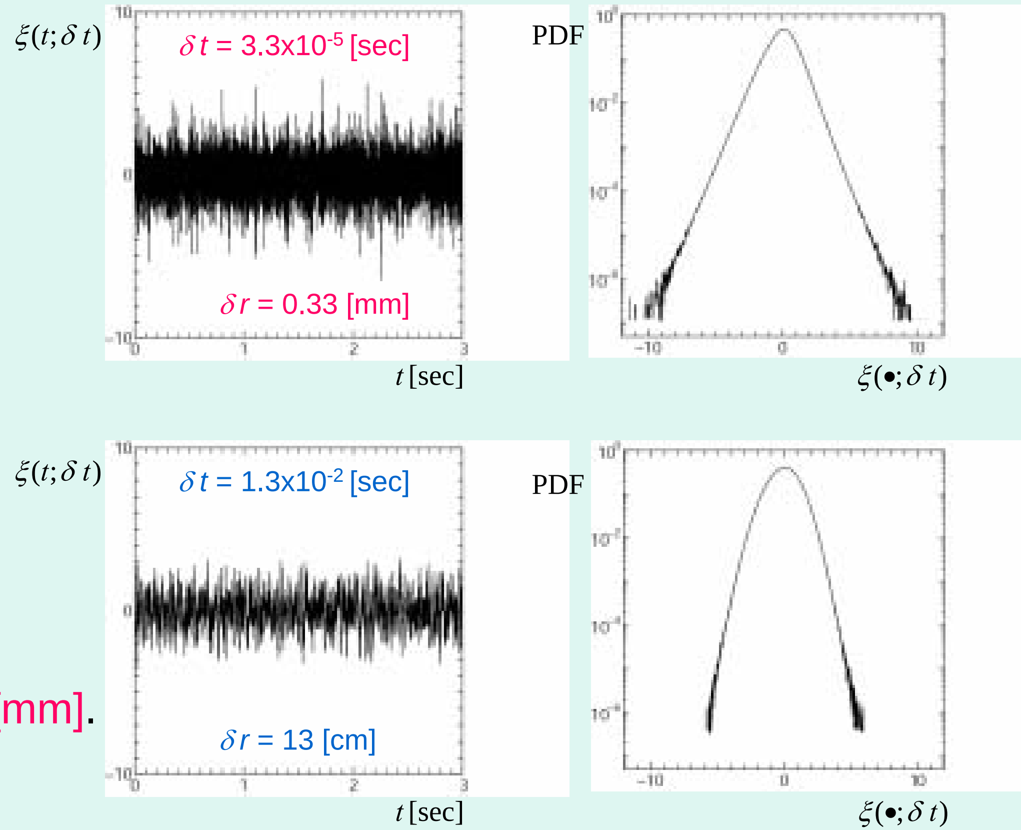

Intermittency in a wind tunnel

Intermittency in the energy dissipation rate ε

$$\varepsilon(x) \approx \nu \left(\frac{\partial u}{\partial x}\right)^2 \propto \left(\frac{\partial u}{\partial t}\right)^2$$

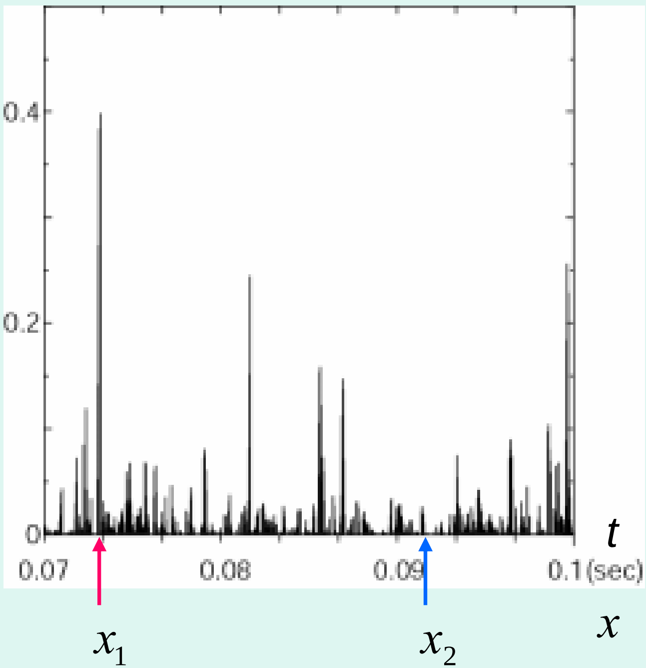

- strongest singularity near x_1
- weakest singularity near x_2

We observe in the energy dissipation rate an intermittent behavior.

We would like to interpret this observation in the following way, i.e., the detector in the wind tunnel measures singularities passing nearby, and their distribution in real space is multifractal following the idear of Frisch and Parisi (1985) and of Meneveau and Sreenivassan (1987).

The method of MFA is constructed under this interpretation.

An experimental “proof” of the existence of singularities

Observation of

fluid particle accelerations

conducted by Bodenschatz et al.

Turbulence chamber (Bodenschatz)

Experiment in a chamber

homogeneous turbulence

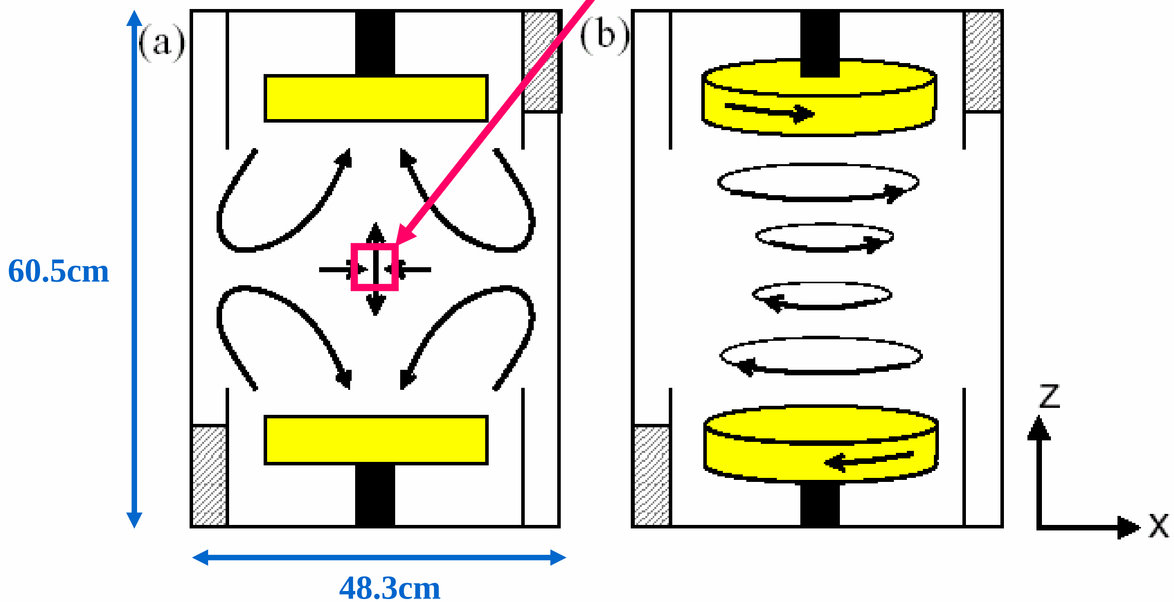

FIGURE 11. Schematic representation of the flow between counter-rotating disks decomposed into (a) the pumping mode and (b) the shearing mode.

Test particle floating in turbulence

Experiment in a chamber

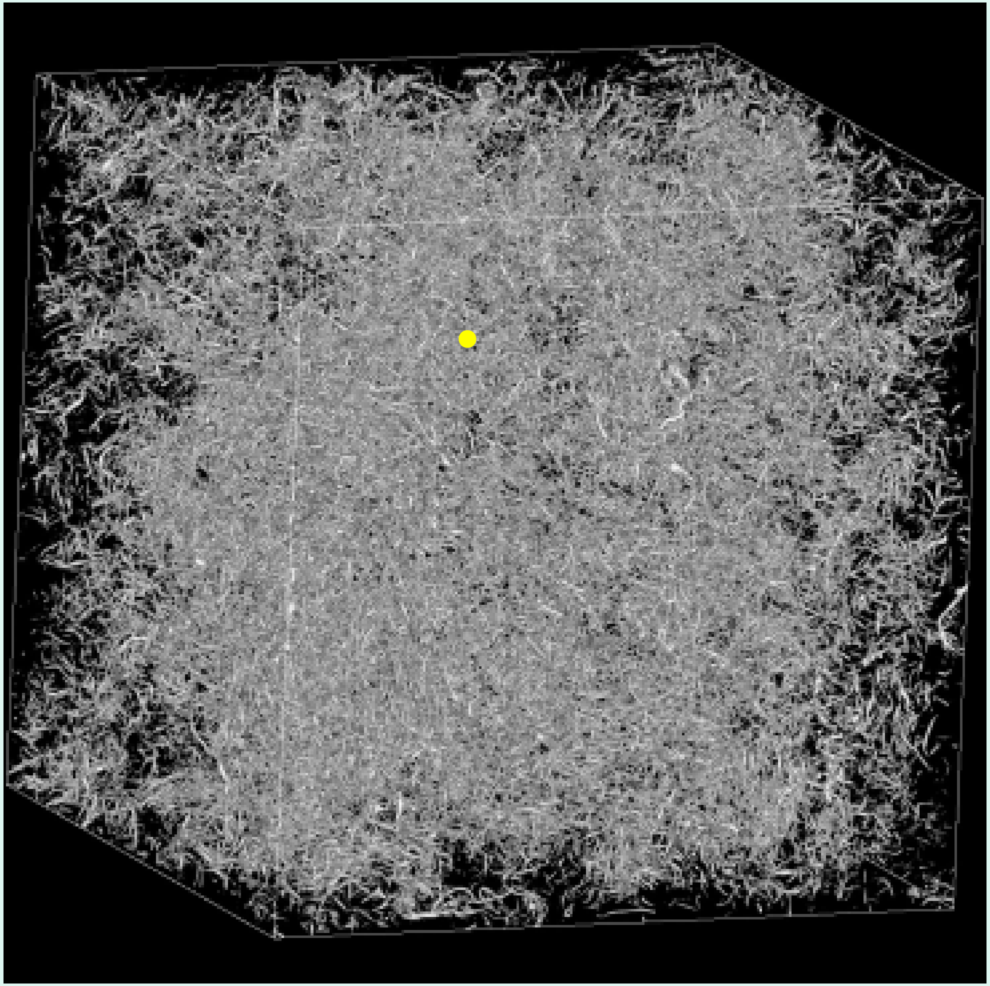

$Q/(u_{\mathrm{rms}}/\ \eta\ )^2 \geq 0.03$, Q : the second invariant of velocity gradient tensor

Trace the trajectory of a 46-μm-diameter test particle in a turbulent water flow.

The test particle is a detector to find out a multifractal distribution of singularities in physical space, which is assumed to be the origin of intermittency.

DNS by M. Tanahashi (TIT) at $Re_\lambda = 220.7$

Experiment in a chamber

Fluid particle accelerations in fully developed turbulence

A. La Porta, Greg A. Voth, Alice M. Crawford, Jim Alexander & Eberhard Bodenschatz

Laboratory of Atomic and Solid State Physics, Laboratory of Nuclear Studies, Cornell University, Ithaca, New York 14853-2501, USA

$R_\lambda = 970$

NATURE | VOL 409 | 22 FEBRUARY 2001 | www.nature.com

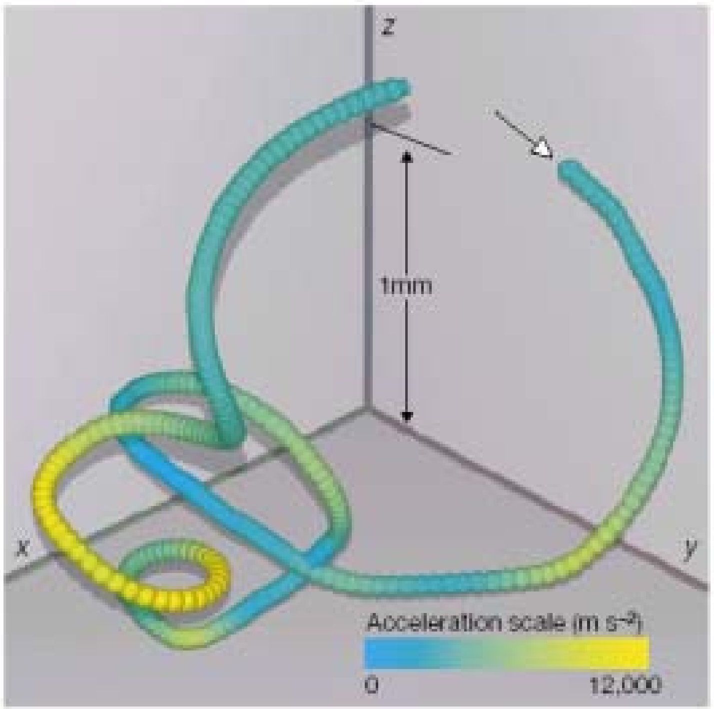

A sphere marks the measured position of the particle in each of 300 frames taken every 0.014 msec ($\sim\tau_\eta/20^{1/2}$).

The shading indicates the acceleration magnitude, with the maximum value of 12,000 msec^{-2} corresponding to ~30 standard deviations.

PDF of accelerations (Bodenschatz)

Experiment in a chamber

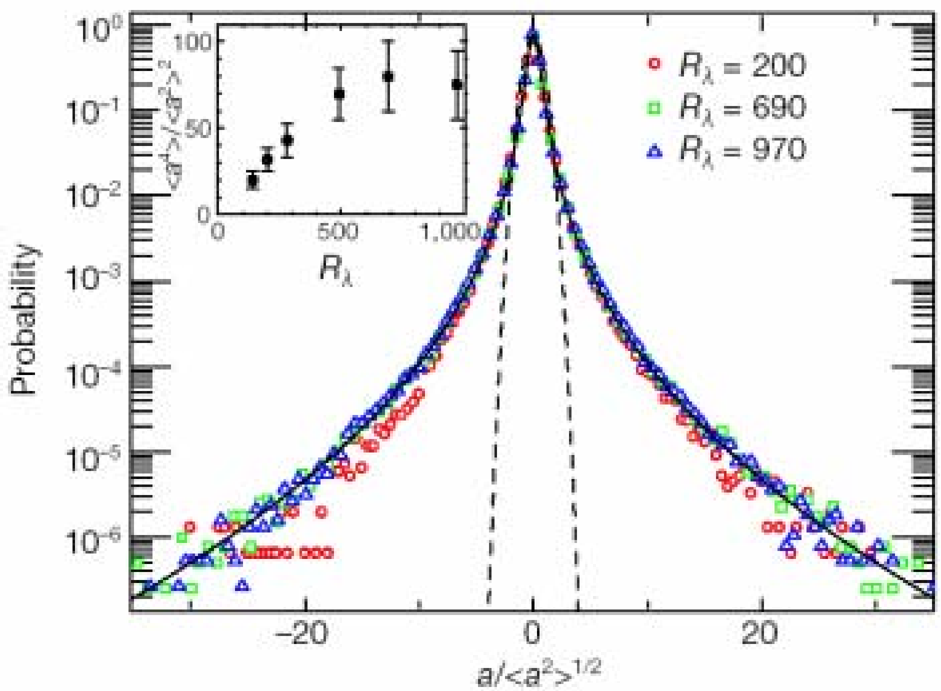

NATURE | VOL 409 | 22 FEBRUARY 2001 | www.nature.com

This observation tells us that turbulence is composed of singularities in physical space. The test particle was kicked by the singularities, and was accelerated so significantly.

Basics
of
Multi-Fractal Analysis
(MFA)

Basics of MFA

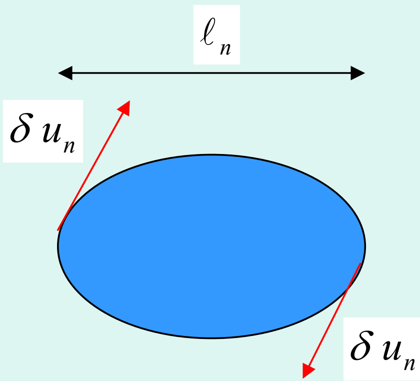

A schematic interpretation

(The eddy of the *n*th generation in the length cascade)

$$\ell_n = \delta_n \ell_0 \quad (\delta_n = 2^{-n})$$

$$E_n = \tfrac{1}{2}\delta u_n^{\ 2} = \int_{k_n}^{k_{n+1}} dk\, E(k) : \text{ kinetic energy per unit mass in scale } \ell_{\mathrm{n}} = k_n^{-1}$$

$$t_n = \ell_n / \delta u_n : \text{ eddy turnover time}$$

$$\varepsilon_{\mathrm{n}} = E_n / t_n \sim \delta u_n^{\ 3} / \ell_n : \text{ energy transfer rate that represents}$$

the rate of transfer of energy per unit mass from eddies of size ℓ_n to those of size ℓ_{n+1}.

Intermittency in terms of Maltifractal Analysis (MFA)

(A&A cond-mat/0306042)

Basics of MFA

- The multifractal analysis (MFA) starts with the scale invariance of the Navier-Stokes equation for high Reynolds number (incompressible fluid).
- "Singularities", due to the invariance, appear in velocity derivatives, pressure gradients (i.e., fluid particle accelerations) and so on, whose degrees of singularity are specified by an exponent α.
- The singularities specified by α are assumed to distribute themselves in physical space with a fractal dimension $f(\alpha)$.
- The probability $P^{(n)}(\alpha)\, d\alpha$, to find a singularity within the range $\alpha \sim \alpha + d\alpha$ at a point in physical space in the nth multifractal depth, is assumed to be specified, once appropriate multifractal spectrum $f(\alpha)$ is given.

Intermittency in terms of Maltifractal Analysis (MFA)

(A&A cond-mat/0306042)

Basics of MFA

- The multifractal analysis (MFA) starts with the scale invariance of the Navier-Stokes equation for high Reynolds number (incompressible fluid).
- "Singularities", due to the invariance, appear in velocity derivatives, pressure gradients (i.e., fluid particle accelerations) and so on, whose degrees of singularity are specified by an exponent α.
- The singularities specified by α are assumed to distribute themselves in physical space with a fractal dimension $f(\alpha)$.
- The probability $P^{(n)}(\alpha)\, d\alpha$, to find a singularity within the range $\alpha \sim \alpha + d\alpha$ at a point in physical space in the nth multifractal depth, is assumed to be specified, once appropriate multifractal spectrum $f(\alpha)$ is given.

Navier-Stokes equation for an incompressible fluid

Basics of MFA

$$\frac{\partial \vec{u}}{\partial t} + \left(\vec{u}\cdot\vec{\nabla}\right)\vec{u} = -\vec{\nabla}\left(\frac{p}{\rho}\right) + \nu\,\nabla^2\vec{u}$$

ρ : the mass density
p : the pressure
ν : the kimenatic viscosity

For high Raynolds number $\mathrm{Re} = \frac{\delta u_0 \ell_0}{\nu} >> 1,$

it is invariant under the scale transformation (α : real)

$$\vec{r} \to \lambda\vec{r},\ \vec{u} \to \lambda^{\alpha/3}\vec{u},\ t \to \lambda^{1-\alpha/3}t,\ \frac{p}{\rho} \to \lambda^{2\alpha/3}\frac{p}{\rho}.$$

Intermittency in terms of Maltifractal Analysis (MFA)

(A&A cond-mat/0306042)

Basics of MFA

- The multifractal analysis (MFA) starts with the scale invariance of the Navier-Stokes equation for high Reynolds number (incompressible fluid).
- "Singularities", due to the invariance, appear in velocity derivatives, pressure gradients (i.e., fluid particle accelerations) and so on, whose degrees of singularity are specified by an exponent α.
- The singularities specified by α are assumed to distribute themselves in physical space with a fractal dimension $f(\alpha)$.
- The probability $P^{(n)}(\alpha)\, d\alpha$, to find a singularity within the range $\alpha \sim \alpha + d\alpha$ at a point in physical space in the nth multifractal depth, is assumed to be specified, once appropriate multifractal spectrum $f(\alpha)$ is given.

"Singularities"

With the length $\ell_n = \delta_n \ell_0 \quad (\delta_n = 2^{-n})$, these quntities are given as follows.

$$|\vec{u}'| = \lim_{n\to\infty} u_n' = \lim_{\ell_n \to 0} \frac{\delta u_n}{\ell_n} \sim \lim_{\ell_n\to 0} \ell_n^{\frac{1}{3}\alpha - 1}, \qquad \delta u_n = | u(\bullet + \ell_n) - u(\bullet) |,$$

$$|\vec{\mathrm{a}}| = \lim_{n\to\infty} \mathrm{a}_n = \lim_{\ell_n \to 0} \frac{\delta p_n}{\ell_n} \sim \lim_{\ell_n\to 0} \ell_n^{\frac{2}{3}\alpha - 1}, \qquad \delta p_n = |(p/\rho)(\bullet + \ell_n) - (p/\rho)(\bullet)|,$$

$$\varepsilon_\infty = \lim_{n\to\infty} \varepsilon_n = \lim_{\ell_n\to 0} \left(\frac{\ell_n}{\ell_0} \right)^{\alpha - 1} \sim \lim_{\ell_n \to 0} \ell_n^{\alpha - 1}$$

where $\vec{\mathrm{a}} = \dfrac{\partial \vec{u}}{\partial t} + (\vec{u} \cdot \vec{\nabla})\, \vec{u}$ is the acceleration of fluid particle.

The velocity derivative, the acceleration and the energy transfer rate become, respectively, singular for $\alpha < 3$, $\alpha < 1.5$ and $\alpha < 1$ in the limit $\ell_n \to 0$.

When $\alpha < 1$, all these three quantities become large for each ℓ_n .

Intermittency in terms of Maltifractal Analysis (MFA)
(A&A cond-mat/0306042)

Basics of MFA

- The multifractal analysis (MFA) starts with the scale invariance of the Navier-Stokes equation for high Reynolds number (incompressible fluid).
- "Singularities", due to the invariance, appear in velocity derivatives, pressure gradients (i.e., fluid particle accelerations) and so on, whose degrees of singularity are specified by an exponent α.
- The singularities specified by α are assumed to distribute themselves in physical space with a fractal dimension $f(\alpha)$.
- The probability $P^{(n)}(\alpha)\, d\alpha$, to find a singularity within the range $\alpha \sim \alpha + d\alpha$ at a point in physical space in the nth multifractal depth, is assumed to be specified, once appropriate multifractal spectrum $f(\alpha)$ is given.

Now, consider Sierpinski's triangular gasket shown in the upper graph of Fig. 3.2. Putting the length of side of the largest "black triangle" ($n = 0$, should appear at the leftmost position in the figure but not shown) be one, we see that the number N_n of triangles appeared at the nth step ($n = 0, 1, 2, \cdots$) is given by

$$N_n = 3^n, \tag{3.6}$$

and that the length δ_n of each side of the triangle by

$$\delta_n = \delta^{-n}, \qquad \delta = 2. \tag{3.7}$$

Then, we know that the total area S_n of the "black trianles" becomes

$$S_n = N_n \frac{3^{1/2}}{4} \delta_n^2 = \frac{3^{1/2}}{4} \left(\frac{3}{4} \right)^n . \tag{3.8}$$

In the limit $n \to \infty$, this area goes down to zero.

Let us regard here that the "black triangles" with area S_n occupies a part of the D dmensional domain with "volume" 1^D, and that the number of D dimensional "boxes" with edge length δ_n necessary to cover the "black triangles" is given by

$$N_n = \frac{1^D}{\delta_n^D} = \delta_n^{-D} = 2^{nD}. \tag{3.9}$$

Equating (3.6) and (3.9), we get

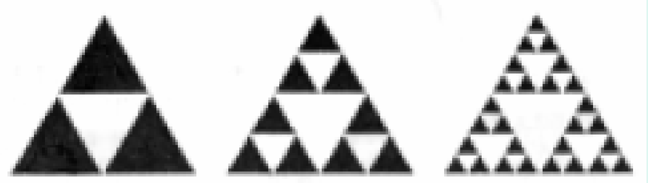

fractal dimension

$$\boxed{D = \frac{\ln 3}{\ln 2} \sim 1.58.}$$

In the case of Sierpinski's carpet given in the lower graph in Fig. 3.2, putting the length of side of the largest "black square" ($n = 0$, should appear at the leftmost position in the figure but not shown) be one, we see that the side length δ_n of each black square in the carpet at the nth step ($n = 1, 2, \cdots$) is given by

$$\delta_n = \delta^{-n}, \qquad \delta = 3, \tag{3.11}$$

and that the number N_n of "black squares" in the carpet by

$$N_n = 8^n. \tag{3.12}$$

Then, we know that the total area S_n of the "black squares" turns out to be

$$S_n = N_n \delta_n^2 = \left(\frac{8}{9}\right)^n. \tag{3.13}$$

In the limit $n \to \infty$, this area also reduces to zero.

Now we consider that the "black squares" of area S_n occupy a part of the D dimansional domain with "volume" 1^D. The number of the D dimensional "boxes" with side length δ_n necessary to cover the "black squares" is given by

$$N_n = \frac{1^D}{\delta_n^D} = \delta_n^{-D} = 3^{nD} \tag{3.14}$$

Equating (3.12) and (3.14), we have

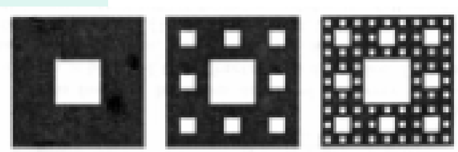

$$\boxed{D = \frac{\ln 8}{\ln 3} \sim 1.89.} \tag{3.15}$$

fractal dimension

Basics of MFA > Fractal <

3.1.3 Probability to Find the Black Reagion

In the previous subsections, we have obtained three fractal dimensions $f(\bullet)$, i.e,

$$f(\text{Koch curve}) = D_{\text{Koch curve}} = 1.26, \tag{3.16}$$

$$f(\text{Sierpinski gasket}) = D_{\text{Sierpinski gasket}} = 1.58, \tag{3.17}$$

$$f(\text{Sierpinski carpet}) = D_{\text{Sierpinski carpet}} = 1.89. \tag{3.18}$$

When one points a box with the side length δ_n on the paper sheet in the regions occupied by the Koch curve, Sierpinski's gasket or carpet, the probability $P_n(\bullet)$ to find the point being "black" at the nth step may be given by the ration between the number $N_n(\bullet)$ of the $f(\bullet)$ dimensional "black" boxes and the total number

$$N_{n,\text{total}} = \frac{1^d}{\delta_n^d} = \delta_n^{-d} \tag{3.19}$$

of boxes in the d-dimansional space, i.e.,

$$P_n(\bullet) = \frac{N_n(\bullet)}{N_{n,\text{total}}} = \delta_n^{d-f(\bullet)}. \tag{3.20}$$

In the present cases, the space is 2-dimensional papser sheet and the probabilities are

$$P_n(\text{Koch curve}) = \delta_n^{2-1.26} = \delta_n^{0.74}, \tag{3.21}$$

$$P_n(\text{Sierpinski gasket}) = \delta_n^{2-1.58} = \delta_n^{0.42}, \tag{3.22}$$

$$P_n(\text{Sierpinski carpet}) = \delta_n^{2-1.89} = \delta_n^{0.11}. \tag{3.23}$$

Basics of MFA

6.2.1 Singularity Distribution

MFA starts with an assignment of the probability, to find a singularity specified by the strength α within the range $\alpha \sim \alpha + d\alpha$, in the form [5, 33]

$$\boxed{P^{(n)}(\alpha)d\alpha = \sqrt{\frac{|f''(\alpha_0)||\ln \delta_n|}{2\pi}}\ \delta_n^{1-f(\alpha)}\ d\alpha.} \tag{6.22}$$

Here, $f(\alpha)$ represents an appropriate multifractal spectrum defined in the range $\alpha_{\min} \leq \alpha \leq \alpha_{\max}$. Note that $f(\alpha)$ does not dependent on n because of the scale invariance.

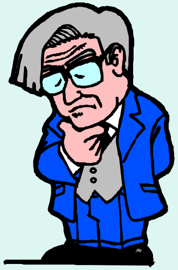

Basics of MFA

The multifractal spectrum is related to the mass exponent $\tau(\bar{q})$, defined by

$$\left\langle \left(\frac{\epsilon_n}{\epsilon} \right)^{\bar{q}} \right\rangle = a_{3\bar{q}}\, \delta_n^{-\tau(\bar{q})+1-\bar{q}} \tag{6.23}$$

with

$$a_{3\bar{q}} = \sqrt{\frac{|f''(\alpha_0)|}{|f''(\alpha_{\bar{q}})|}}, \tag{6.24}$$

through the Legendre transformation [33]:

$$\boxed{f(\alpha) = \alpha\bar{q} + \tau(\bar{q})} \tag{6.25}$$

with

$$\alpha = \alpha_{\bar{q}} = -\frac{d\tau(\bar{q})}{d\bar{q}} \tag{6.26}$$

and

$$\bar{q} = \frac{df(\alpha)}{d\alpha}. \tag{6.27}$$

The average $\langle \cdots \rangle$ is taken with $P^{(n)}(\alpha)$, and $\alpha_0 = \alpha_{\bar{q}=0} = \langle \alpha \rangle$.

Basics of MFA

The scaling exponent ζ_m of the mth order velocity structure function, defined by

$$\langle |u_n|^m \rangle \propto \delta_n^{\ \zeta_m}, \tag{6.28}$$

is related to the mass exponent by

$$\boxed{\zeta_m = 1 - \tau\left(\frac{m}{3}\right).} \tag{6.29}$$

This is derived with the help of (6.9) and (6.18) as

$$\langle |u_n|^m \rangle = \delta_n^{m/3} \left\langle \left(\frac{\epsilon_n}{\epsilon}\right)^{m/3} \right\rangle = a_m \delta_n^{\ 1-\tau(m/3)}. \tag{6.30}$$

Basics of MFA

Distribution of α is essential to determine ζ_m.

- $P^{(n)}(\alpha)$: distribution for α
  $\to f(\alpha)$: multifractal spectrum
- $\tau(\bar{q})\left(= f(\alpha) - \alpha\bar{q}\right)$: mass exponent
  $\to \varsigma_m \left(= 1 - \tau(m/3)\right)$: scaling exponents of VSF
- Choice of $P(\alpha)$

  P model: Binomial distribution

  Log-normal model: Gaussian distribution

  A&A model: Tsallis-type distribution

Structure of PDFs within MFA

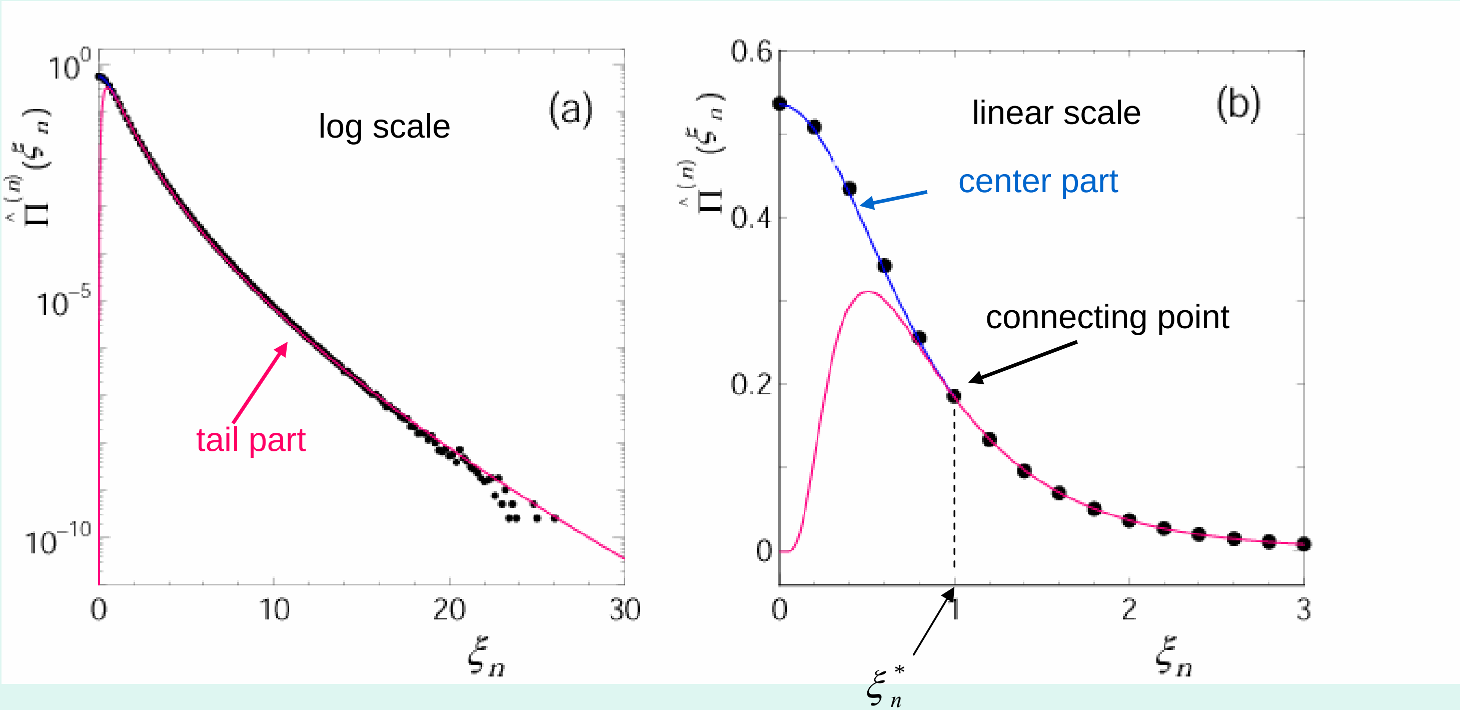

It is revealed in the analyses of experimental data that there are two mechanisms contributing to the PDFs, i.e,

- one is for the **tail part**, and
- the other for the **center part**.

Basics of MFA

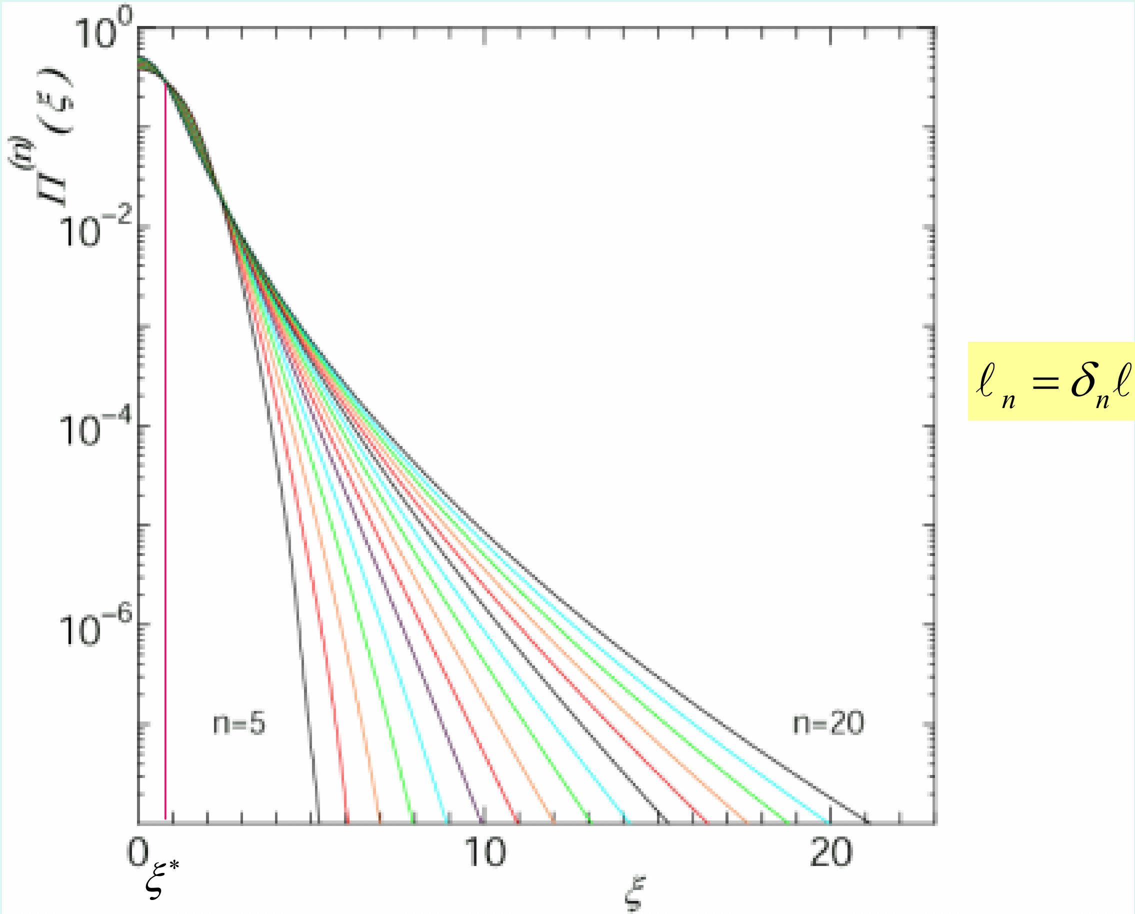

$$\ell_n = \delta_n \ell_0 \quad (\delta_n = 2^{-n})$$

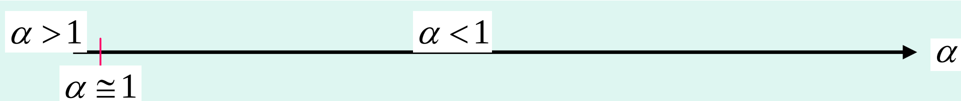

Basics of MFA

Tail part

- The structure of the tail part represents the intermittent large deviations,
  - which is a manifestation of the multifractal distribution of singularities in physical space due to the scale invariance of the Navier-Stokes equation for large Reynolds number.
- The specific form of the tail part comes from the distribution function $P^{(n)}(\alpha)$ for the singularity exponent α, that is represented by

$$\hat{\Pi}_{\phi}^{(n)}(|\xi_n|)\,d|\xi_n| = \Pi_{\phi,\mathrm{S}}^{(n)}(|x_n|)\,d|x_n| = \frac{1-2\gamma_{\phi,0}^{(n)}}{2}\,P^{(n)}(\alpha)\,d\alpha$$

$$|x_n| = \delta_n^{\phi\alpha/3},$$

$$\xi_n = \frac{x_n}{\sqrt{\langle\langle |x_n|^2 \rangle\rangle}} = \frac{x_n'}{\sqrt{\langle\langle (x_n')^2 \rangle\rangle}}$$

  - P model: Binomial distibution
  - Log-normal: Gaussian distribution
  - A&A model: Tsallis-type distribution with the parameters which are determined by the observed value of the intermittency exponent μ.
  - Note that the parameter q in A&A model does not depend on the distance r between two observation points.

Basics of MFA

Center part

- The structure of the center part represents small deviations
  - violating the scale invariance mainly due to thermal fluctuations.
- The center part is assumed to be given by
  - the Tsallis-type distribution function for the variable ξ_n itself with the parameter q'.
  - q' depends on the distance r between two observation points.
  - The dependence is extracted through the study of the PDF's of velocity fluctuations.

$$\hat{\Pi}_{\phi}^{(n)}(\xi_n)d\xi_n = \left[\Pi_{\phi,\mathrm{S}}^{(n)}(x_n) + \Delta\Pi_{\phi}^{(n)}(x_n)\right] dx_n$$

$$= \bar{\Pi}_{\phi}^{(n)} \left\{1 - (1-q')\frac{(\phi + 3f'(\alpha^*))}{2\phi}\left[\left(\frac{\xi_n}{\xi_n^*}\right)^2 - 1\right]\right\}^{1/(1-q')} d\xi_n$$

Extraction of singularities out of time series data

Extraction of singularities

Let us introduce the total dissipation rate $\mathcal{E}_n$ at the nth step $(d=1)$ by

$$\mathcal{E}_n = \epsilon_n \ell_n \tag{7.1}$$

and its generating function $\mathcal{Z}_n$ per unit length by

$$\boxed{\mathcal{Z}_n = \left\langle \left(\frac{\mathcal{E}_n}{\mathcal{E}_0} \right)^{\bar{q}} \right\rangle \delta_n^{-1} = a_{3\bar{q}}\ \delta_n^{-\tau(\bar{q})} = a_{3\bar{q}}\ \delta_n^{(\bar{q}-1)D_{\bar{q}}}} \tag{7.2}$$

where we used (5.23) and the definition of the generalized dimension (3.48).

Since the dissipation rate ϵ_n is proportional to the square of the velocity derivative at the nth step, i.e.,

$$\epsilon_n \propto \nu \left(u_n' \right)^2 , \tag{7.3}$$

we can extract the generalized dimension $D_{\bar{q}}$ from the experimental data of velocity derivative. Furthermore, with the help of Taylor's frozen hypothesis, the velocity derivative is proportional to the time derivative of velocity field. Therefore, we see that the generalized dimension can be estimated from the time series data of velocity field through (7.2).

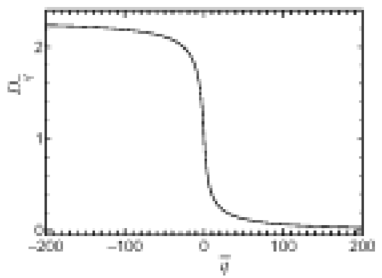

Fig. 5.2. Generalized dimension $D_{\bar{q}}$ with $\mu = 0.240$ ($q = 0.391$).

Intermittency in the energy dissipation rate ε

Extraction of singularities

$$\varepsilon(x) \approx \nu\left(\frac{\partial u}{\partial x}\right)^2 \propto \left(\frac{\partial u}{\partial t}\right)^2$$

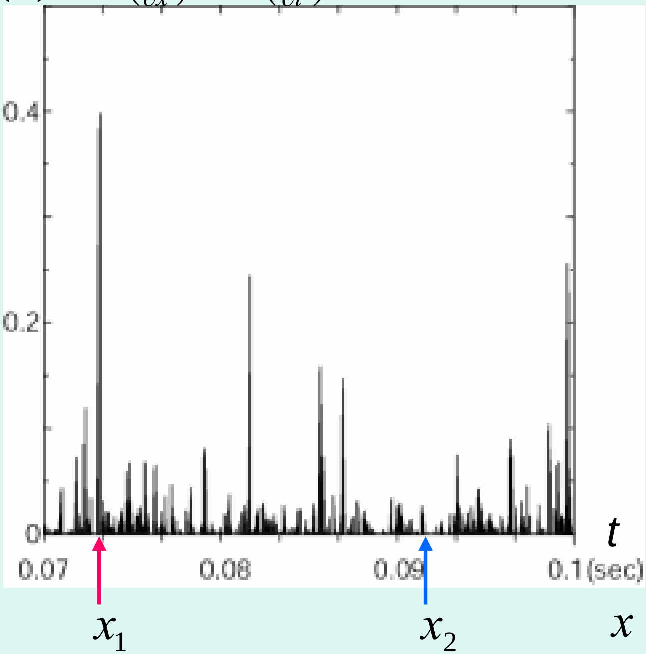

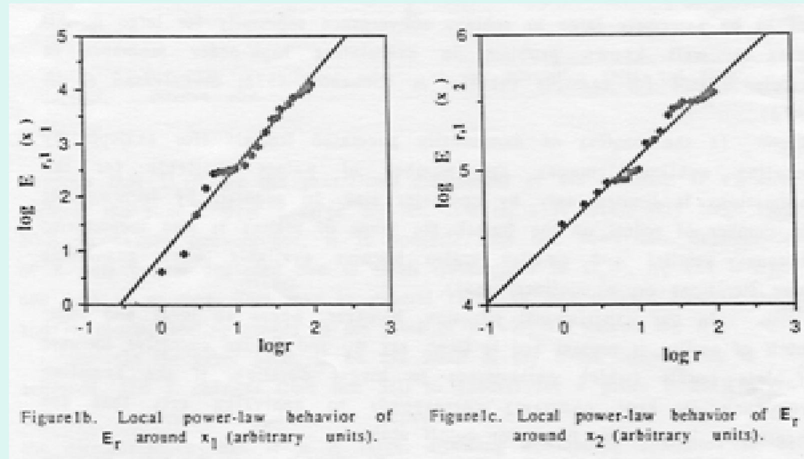

From Z_n we can extract D_q.

$$\tau(\bar{q}) = (1 - \bar{q}) D_{\bar{q}},$$

$$f(\alpha) = \alpha\bar{q} + \tau(\bar{q})$$

$$\alpha = \alpha_{\bar{q}} = -\frac{d\tau(\bar{q})}{d\bar{q}}$$

$$\bar{q} = \frac{df(\alpha)}{d\alpha}.$$

P Model

P model

The distribution function $P^{(n)}(\alpha)$ for the p model [29, 33] is specified based on the binomial multiplicative process in the form [1]

$$\boxed{P^{(n)}(\alpha) = \frac{1}{Z_0^{(n)}} \frac{1}{[2y^y(1-y)^{1-y}]^n}} \tag{6.87}$$

with

$$y = y(\alpha) = \frac{\alpha + \log_2(1-p)}{\log_2[(1-p)/p]} \tag{6.88}$$

and the partition function

$$Z_0^{(n)} = \sqrt{\frac{\pi}{2n}} \log_2\left(\frac{1-p}{p}\right) \tag{6.89}$$

for $n \gg 1$.

The multifractal spectrum is given by

$$\boxed{f(\alpha) = -\{y(\alpha)\log_2 y(\alpha) + [1-y(\alpha)]\log_2[1-y(\alpha)]\},} \tag{6.90}$$

which leads to the mass exponent

$$\boxed{\tau(\bar{q}) = \log_2\left[p^{\bar{q}} + (1-p)^{\bar{q}}\right].} \tag{6.91}$$

P model

The parameter p are determined by the conditons

$$\left\langle \left(\varepsilon_n / \varepsilon \right)^2 \right\rangle = \delta_n^{-\mu}.$$

Note that $\langle \cdots \rangle$ is taken with $P^{(n)}(\alpha)$.

$$p = \frac{1 + \sqrt{2^\mu - 1}}{2}.$$

Log-Normal Model

Log-normal model

In the log-normal model [18–20], one consider the ratio $\epsilon_n/\epsilon_{n-1}$ $(n = 1, 2, \cdots)$ as independent stochastic variables, and apply for $n \gg 1$ the central limit theorem to the summation of their logarithms,

$$\boxed{\frac{1}{\sqrt{n\sigma^2}} \sum_{j=1}^{n} \ln\left(\frac{\epsilon_j}{\epsilon_{j-1}}\right) = \frac{1}{\sqrt{n\sigma^2}} \ln\left(\frac{\epsilon_n}{\epsilon}\right) = \sqrt{\frac{n}{\sigma^2}}\,(1-\alpha)\ln\delta,} \tag{6.74}$$

to have the Gaussian distribution function

$$\boxed{P^{(n)}(\alpha) = \sqrt{\frac{n}{2\pi\sigma^2}}\; \mathrm{e}^{-n(\alpha-\alpha_0)^2/2\sigma^2}} \tag{6.75}$$

for the range $-\infty < \alpha < \infty$. Here, we used the scaling relation (6.18) between ϵ_n and α. Then, we have the multifractal spectrum and the mass exponent in the forms

$$f(\alpha) = 1 - \frac{(\alpha-\alpha_0)^2}{2\sigma^2 \ln\delta} \tag{6.76}$$

and

$$\tau(\bar{q}) = 1 - \alpha_0 \bar{q} + \frac{1}{2}\bar{q}^2\sigma^2 \ln\delta, \tag{6.77}$$

respectively. We see that

$$a_{3\bar{q}} = 1. \tag{6.78}$$

Log-normal model

Two parameters α_0, σ are determined by the conditons

$$\underline{\langle \varepsilon_n / \varepsilon \rangle = 1}, \quad \underline{\left\langle (\varepsilon_n / \varepsilon)^2 \right\rangle = \delta_n^{-\mu}}.$$

Note that $\langle \cdots \rangle$ is taken with $P^{(n)}(\alpha)$.

$$\alpha_0 = 1 + \frac{\mu}{2} \tag{6.79}$$

and

$$\sigma^2 = \frac{\mu}{\ln \delta}. \tag{6.80}$$

Then, we have

$$\boxed{f(\alpha) = 1 - \frac{(\alpha - \alpha_0)^2}{2\mu}} \tag{6.81}$$

and

$$\boxed{\tau(\bar{q}) = (1 - \bar{q}) D_{\bar{q}}} \tag{6.82}$$

with the generalized dimension

$$D_{\bar{q}} = 1 - \mu \bar{q}/2, \tag{6.83}$$

which are the same as derived in [33]. We know that

$$\alpha_{\bar{q}} = \alpha_0 - \mu \bar{q}. \tag{6.84}$$

A&A Model

Gibbs statistics

A&A model >Gibbs<

$$S = -\sum_i p_i \ln p_i$$

$$\sum_i p_i = 1,\ U = \sum_i p_i E_i$$

Thermal equilibrium distribution function

$$p_i = \mathrm{e}^{-\beta E_i} / Z,\ Z = \sum_i \mathrm{e}^{-\beta E_i}$$

Renyi statistics

A&A model >Renyi<

$$S_q = \frac{1}{1-q} \ln\left(\sum\nolimits_i p_i^q\right)$$

$$\sum_i p_i = 1, \; U_q = \frac{\sum_i p_i^q E_i}{\sum_i p_i^q}$$

Stationary state distribution function

$$p_i = \frac{1}{\bar{Z}_q} \left[1-(1-q)\beta(E_i - U_q)\right]^{1/(1-q)}$$

$$\bar{Z}_q = \sum_i \left[1-(1-q)\beta(E_i - U_q)\right]^{1/(1-q)}$$

q → 1 gives us the Gibbs.

Additive

A&A model >Renyi<

$$S_q(A+B) = S_q(A) + S_q(B)$$

Havrda-Charvat-Tsallis statistics

A&A model >Tsallis<

$$S_q = \frac{\sum_i p_i^q - 1}{1-q}$$

$$\sum_i p_i = 1, \; U_q = \frac{\sum_i p_i^q E_i}{\sum_i p_i^q}$$

Stationary state distribution function

$$p_i = \frac{1}{\overline{Z}_q}\left[1 - \frac{(1-q)\beta(E_i - U_q)}{\overline{Z}_q^{1-q}}\right]^{1/(1-q)}$$

$$\overline{Z}_q = \sum_i \left[1 - \frac{(1-q)\beta(E_i - U_q)}{\overline{Z}_q^{1-q}}\right]^{1/(1-q)}$$

q → 1 gives us the Gibbs.

Pseudo-additivity

$$S_q(A+B) = S_q(A) + S_q(B) + (1-q)S_q(A)S_q(B)$$

A&A model

Taking an extremum of the generalized entropy

$$S_q[P(\alpha)] = \left[\int d\alpha\, P(\alpha)^q - 1\right] \Big/ (1-q) \quad \text{(Tsallis)}$$

$$S_q[P(\alpha)] = \left[\ln \int d\alpha\, P(\alpha)^q\right] \Big/ (1-q) \quad \text{(Renyi)}$$

with the constraints

$$\int d\alpha\, P(\alpha) = \text{const}, \quad \int d\alpha\, P(\alpha)^q (\alpha - \alpha_0)^2 \Big/ \int d\alpha\, P(\alpha)^q = \sigma_q{}^2,$$

we have

$$\boxed{P^{(n)}(\alpha) = [P(\alpha)]^n = \frac{1}{Z^{(n)}} \left[1 - \frac{(\alpha-\alpha_0)^2}{(\Delta\alpha)^2}\right]^{n/(1-q)}}$$

with $(\Delta\alpha)^2 = \dfrac{2X}{(1-q)\ln 2}$ and $\sigma_q{}^2 = \dfrac{2X}{(3-q)\ln 2}$.

The multifractal spectrum can be extracted as $(P^{(n)}(\alpha) \propto \delta_n^{1\text{-}f(\alpha)})$

$$\boxed{f(\alpha) = 1 - \frac{1}{1-q} \log_2 \left[1 - \frac{(\alpha-\alpha_0)^2}{(\Delta\alpha)^2}\right]}$$

The parameters q, α_0, X are to be determined.

Havrda-Charvat-Tsallis type distribution function

A&A model

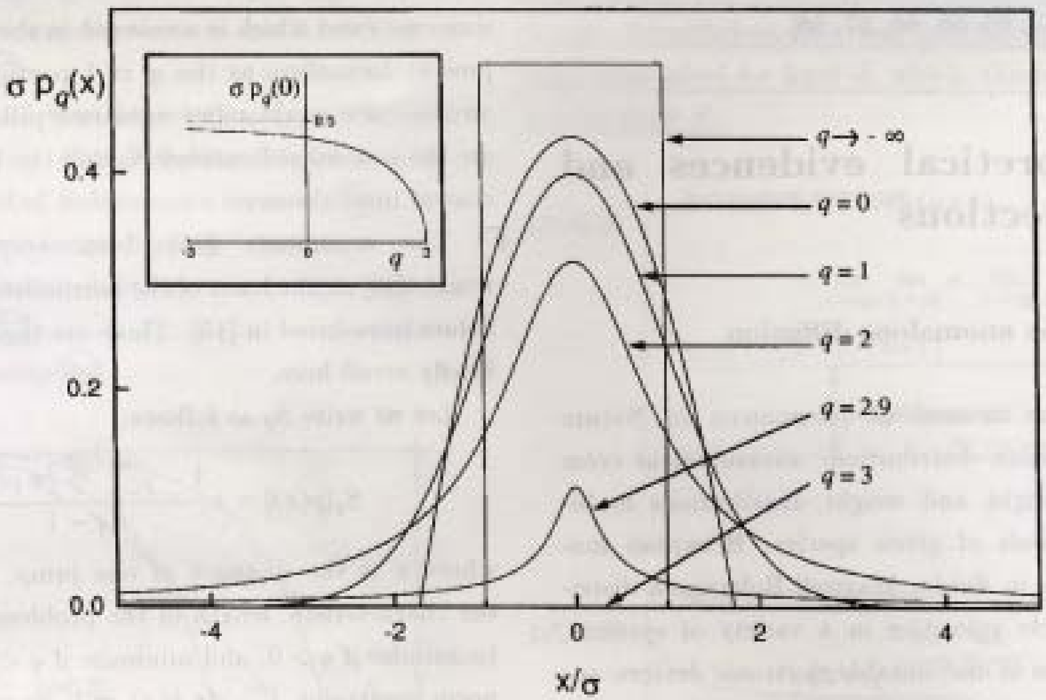

Figure 5. The one-jump distributions $p_q(x)$ for typical values of q. The $q \to -\infty$ distribution is the uniform one in the interval $[-1,1]$; $q=1$ and $q=2$ respectively correspond to Gaussian and Lorentzian distributions; the $q \to 3$ is completely flat. For $q<1$ there is a cut-off at $|x|/\sigma = [(3-q)/(1-q)]^{1/2}$.

A&A model

A&A model assumes that the distribution of α is given by the Havrda-Charvat-Tsallis (HCT) type distribution function

$$P^{(n)}(\alpha) = \frac{1}{Z^{(n)}}\left[1 - \frac{(\alpha-\alpha_0)^2}{(\Delta\alpha)^2}\right]^{n/(1-q)}$$

with $(\Delta\alpha)^2 = 2X/(1-q)\ln 2$. Then, the multifractal spectrum has the form

$$f(\alpha) = 1 - \frac{1}{1-q}\log_2\left[1 - \frac{(\alpha-\alpha_0)^2}{(\Delta\alpha)^2}\right]$$

Three parameters α_0, X, q are determined by the conditons

$$\langle \varepsilon_n/\varepsilon \rangle = 1, \quad \left\langle (\varepsilon_n/\varepsilon)^2 \right\rangle = \delta_n^{-\mu}, \quad \frac{1}{1-q} = \frac{1}{\alpha_-} - \frac{1}{\alpha_+}.$$

$$f(\alpha_\pm) = 0$$

Note that $\langle \cdots \rangle$ is taken with $P^{(n)}(\alpha)$.

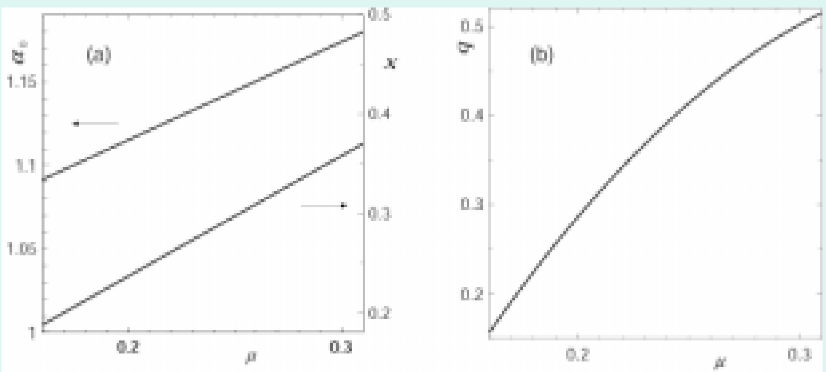

A generalization of the scaling relation proposed by Lyra & Tsallis (1998).

A&A model

The PDF $\hat{\Pi}_{\phi}^{(n)}(\xi_n)d\xi_n = \Pi_{\phi}^{(n)}(x_n)dx_n$ for quqntity x_n with the normalized variable $\xi_n = x_n \Big/ \sqrt{\langle\langle x_n{}^2 \rangle\rangle}$ is given by

$$\hat{\Pi}_{\phi}^{(n)}(\xi_n) = \overline{\Pi}_{\phi}^{(n)} \left\{1 - \frac{(1-q')\left[1+3f'(\alpha^*)/\phi\right]}{2}\left[(\xi_n/\xi_n{}^*)^2 - 1\right]\right\}^{1/(1\text{-}q')} \quad \text{for } |\xi_n| \le \xi_n{}^* \quad (\alpha \ge \alpha^*)$$

$$\hat{\Pi}_{\phi}^{(n)}(\xi_n) = \overline{\Pi}_{\phi}^{(n)} \frac{\bar{\xi}_n}{|\xi_n|}\left[1 - \frac{1-q}{n}\frac{\left(3\ln|\xi_n/\xi_{n,0}|\right)^2}{2\phi^2 X|\ln\delta_n|}\right]^{n/(1-q)} \quad \text{for } \xi_n{}^* \le |\xi_n| \quad (\alpha^* \ge \alpha)$$

with $|\xi_{n,0}| = \bar{\xi}_n \delta_n{}^{2\alpha_0/3 - \zeta_{2\phi}/2}$.

HCT-type distribution function representing not a simple power law

- ϕ =1: velocity fluctuations and derivatives
- ϕ =2: fluid particle accelerations
- ϕ =3: energy transfer rates

The connection point $\xi_n{}^* (\approx 0.5 \sim 1.4)$ is defined by $\xi_n{}^* = \bar{\xi}_n \delta_n^{2\alpha^*/3 - \zeta_{2\phi}/2}$.

Here, $\alpha^* \approx 1.0 \sim 1.1$ is the solution of $\zeta_{2\phi}/2 - \phi\alpha/3 + 1 - f(\alpha) = 0$.

ς_m is the scaling exponent of velocity structure function.

Remember that variables become singular for $\alpha < 1$.

Comparison in ζ_m

Scaling exponents ζ_m of velocity structure function

Comparison

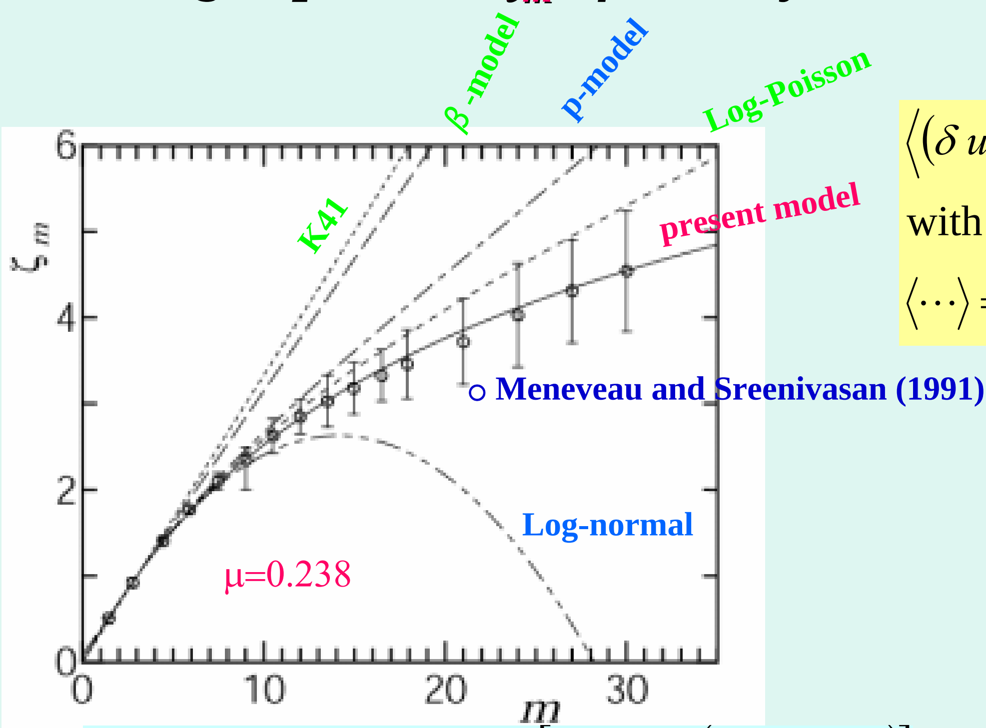

$$\left\langle \left(\delta u_n\right)^m \right\rangle \propto \ell_n^{\zeta_m}$$

with $\delta u_n = \left| u(\bullet + \ell_n) - u(\bullet) \right|$,

$$\langle \cdots \rangle = \int d\alpha \cdots P(\alpha).$$

$$\zeta_m = \frac{\alpha_0 m}{3} - \frac{2X m^2}{9(1+\sqrt{C_{m/3}})} - \frac{1}{1-q}\left[1 - \log_2\left(1+\sqrt{C_{m/3}}\right)\right]$$

with

present model (2000)

$$C_{\bar{q}} = 1 + 2X\,\bar{q}^2(1-q)\ln 2$$

$$\sqrt{2X} = \frac{\sqrt{\alpha_0^2 + (1-q)^2} - (1-q)}{\sqrt{b}}, \quad b = \frac{1-2^{q-1}}{(1-q)\ln 2}.$$

K41 (1941)

$\zeta_m = m / 3$

Log-normal (1962)

$\zeta_m = m / 3 - \mu\, m(m-3) / 18$

β -model (1978)

$\zeta_m = m / 3 - \mu\,(m-3) / 3$

p-model (1987)

$\zeta_m = 1 - \log_2 [p^{m/3} + (1-p)^{m/3}]$

$p = (1 + (2^{\mu} - 1)^{1/2})/2$

Log-Poisson (1994)

$\zeta_m = m / 9 + 2(1 - (2/3)^{m/3})$

Analysis of experiment conducted by Bodenschatz el al.

PDF of fluid particle accelerations

Let us analyze the PDF of particle accelerations observed by Bodenschatz at R_λ=690.

Bodenschatz

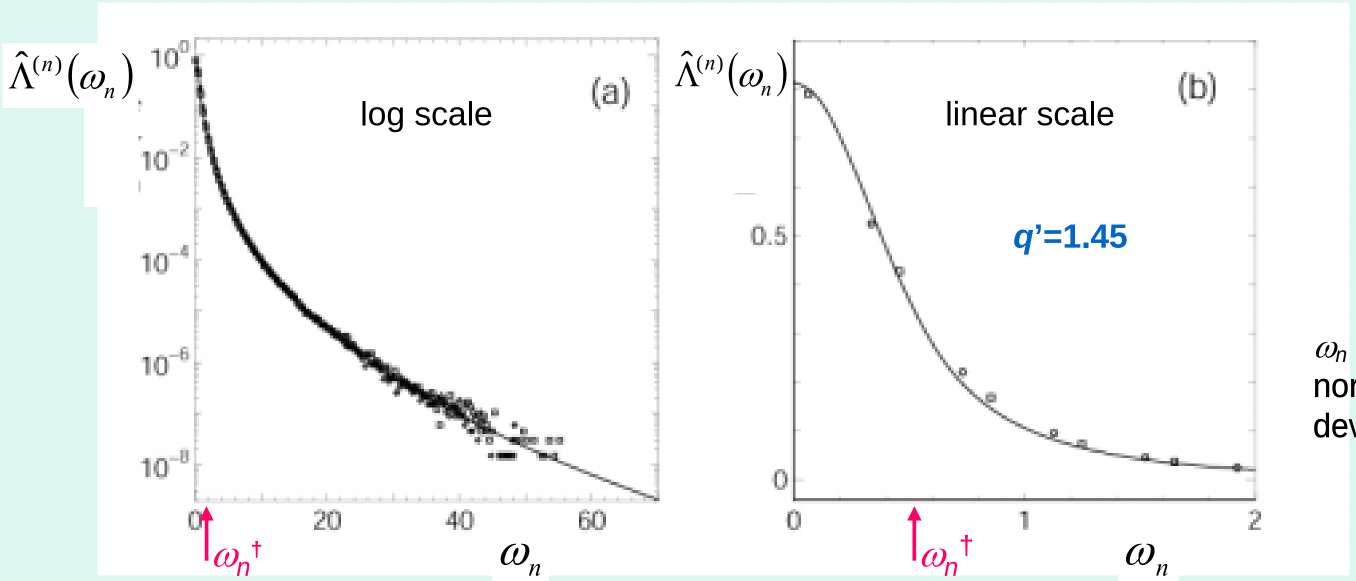

ω_n : acceleration normalized by its deviation

<u>Open squares and circles</u>
Experimental PDF by Bodenschatz et.al (2002)

<u>Lines</u>
Theoretical PDF with q= 0.391 (μ= 0.240) by AA (2002)

$\omega_n^\dagger$= 0.550 $\alpha^\dagger$= 1.01 n = 17.1

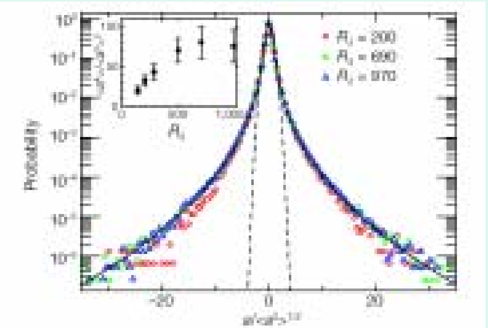

Analysis of DNS conducted by Gotoh et al.

PDF of fluid particle accelerations

PDF of velocity fluctuations

PDF of fluid particle accelerations (Gotoh)

Gotoh

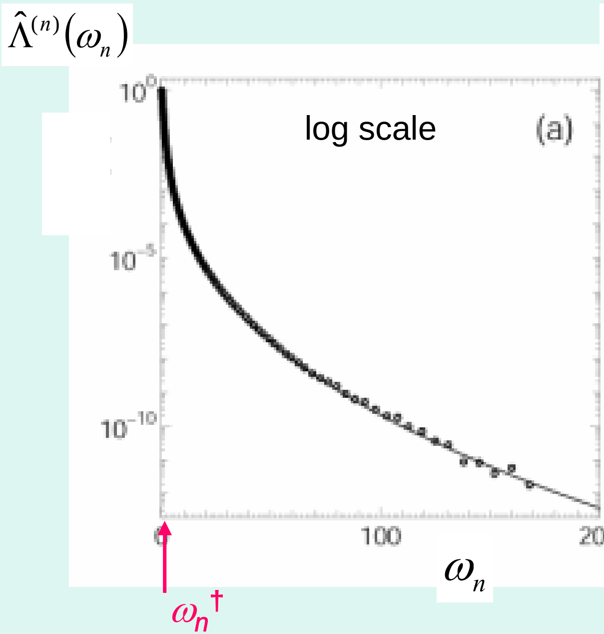

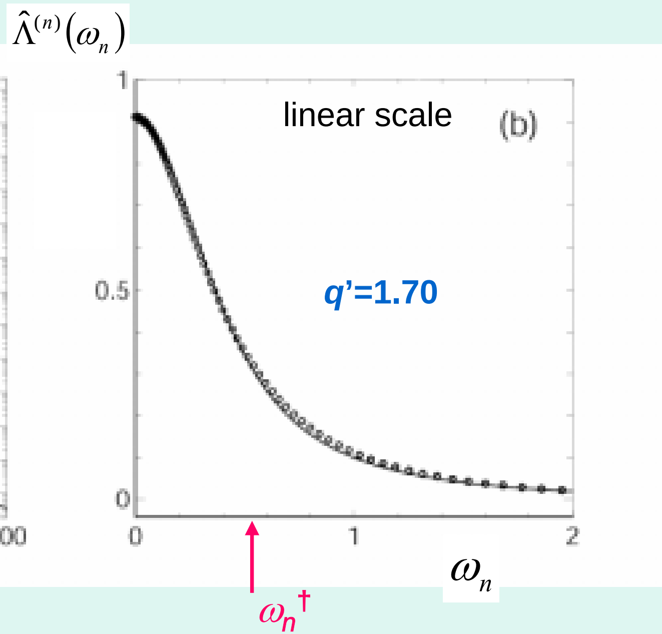

ω_n : acceleration normalized by its deviation

Open squares and circles

Experimental PDF by Gotoh et al. (2002)

Lines

Theoretical PDF with q = 0.391 (μ =0.240) by AA (2002)

$\omega_n^\dagger$ = 0.550 $\alpha^\dagger$= 1.01 n = 17.5

Measurement of velocity fluctuations

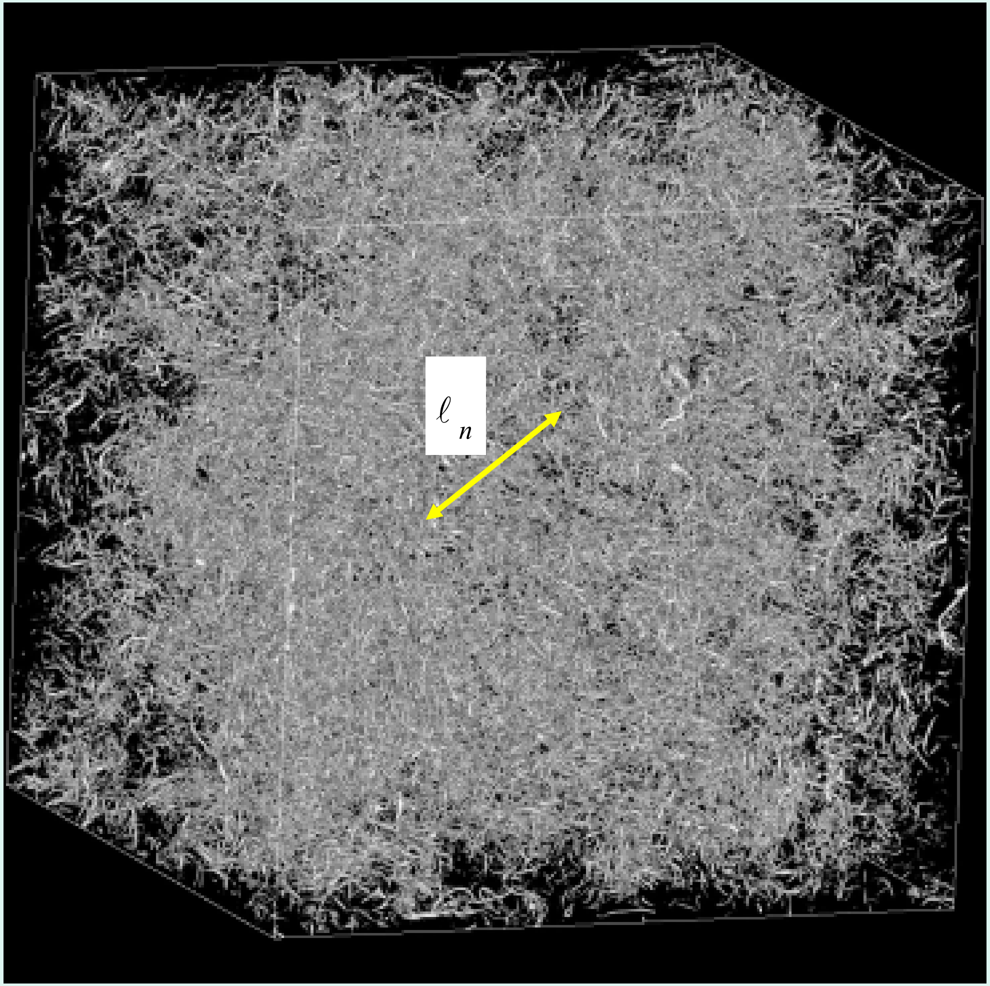

The velocity fluctuation is measured at every two points separated by ℓ_n.

$$Re_\lambda = 220.7$$

by M. Tanahashi (TIT)

$Q/(u_{\rm rms}/\eta)^2 \geq 0.03$, Q : the second invariant of velocity gradient tensor

PDF of velocity differences (Gotoh)

Gotoh

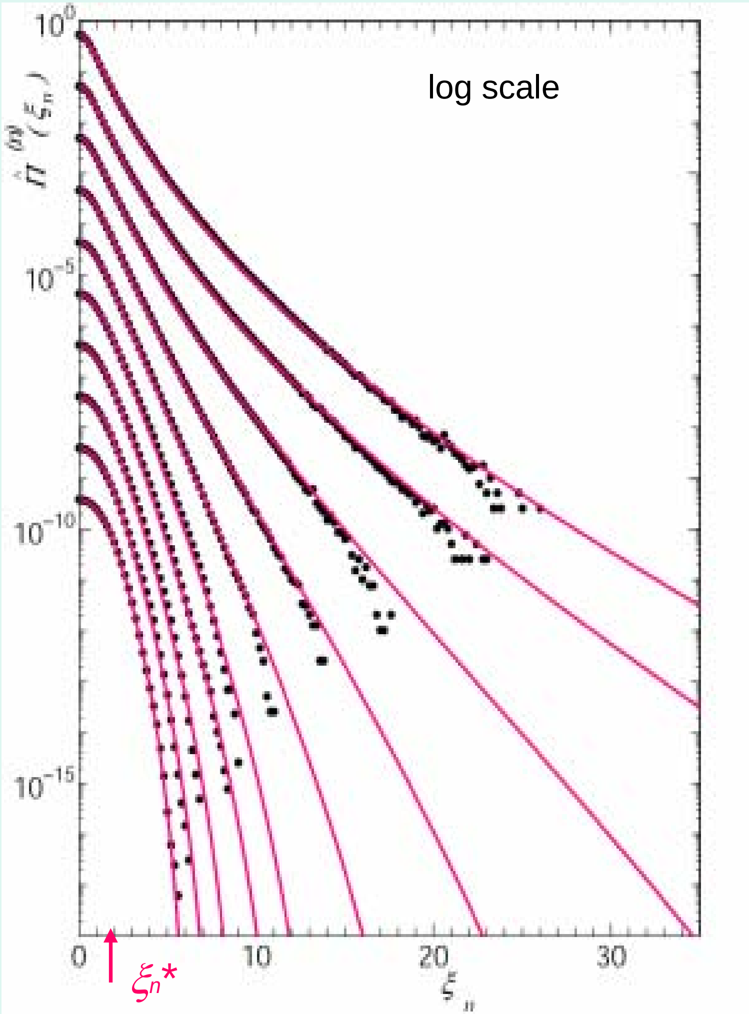

<u>Closed circles</u>

Experimental PDF by Gotoh et al. (2002)

r/η from top to bottom:
2.38, 4.76, 9.52, 19.0, 38.1, 76.2, 152, 305, 609, 1220

<u>Lines</u>

Theoretical PDF with q = 0.391 (μ =0.240) by AA (2001)

n from top to bottom:
20.7, 19.2, 16.2, 13.6, 11.5, 9.80, 9.00, 7.90, 7.00, 6.00

$\xi_n{}^*$ from top to bottom:
1.10, 1.13, 1.19, 1.23, 1.28, 1.32, 1.34, 1.37, 1.39, 1.43

q' from top to bottom:
1.60, 1.60, 1.58, 1.49, 1.45, 1.40, 1.35, 1.30, 1.25, 1.20

α^*= 1.07

n: number of multifractal steps

For better visibility, each PDF is shifted by –1 unit along the vertical axis.

ξ_n : velocity fluctuation normalized by its deviation

PDF of velocity differences (Gotoh)
Central Part

Goto h

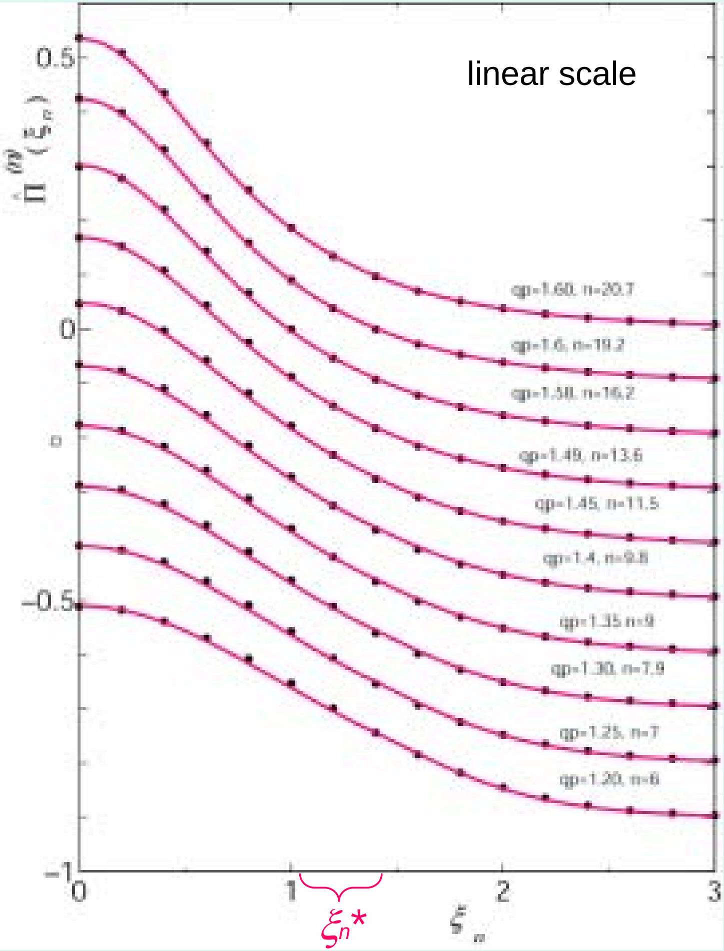

<u>Closed circles</u>
Experimental PDF by Gotoh et al. (2002)
r/η from top to bottom:
2.38, 4.76, 9.52, 19.0, 38.1, 76.2, 152, 305, 609, 1220

<u>Lines</u>
Theoretical PDF with q = 0.391
(μ =0.240) by AA (2001)
n from top to bottom:
20.7, 19.2, 16.2, 13.6, 11.5, 9.80, 9.00, 7.90, 7.00, 6.00
ξ_n^* from top to bottom:
1.10, 1.13, 1.19, 1.23, 1.28, 1.32, 1.34, 1.37, 1.39, 1.43
q' from top to bottom:
1.60, 1.60, 1.58, 1.49, 1.45, 1.40, 1.35, 1.30, 1.25, 1.20
α^*= 1.07
n: number of multifractal steps

For better visibility, each PDF is shifted by –1 unit along the vertical axis.

Competion among multifractal models

P model, Log-normal model, A&A model

Competition in ζ_m

P model, Log-normal model, A&A model

Competition I

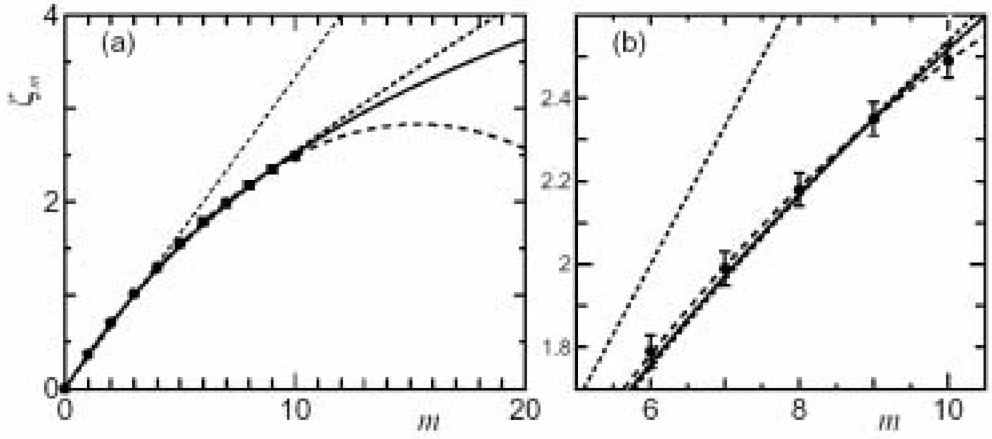

Fig. 6.4. Analysis of the scaling exponents ζ_m of velocity structure function extracted from the DNS conducted by Gotoh et al. by the present theoretical curve (solid line). Those by K41 (dotted line), the log-normal model (dashed line) and the p model (dotted-dashed line) are also shown for comparison.

The scaling exponents ζ_m of velocity structure function reported by Gotoh et al. [27] are analyzed in Fig. 6.4 by the method of the least squares (MLS) with the theoretical formulae of the harmonious representation, of the log-normal model and of the p model, giving, respectively, the values of the intermittency exponent $\mu = 0.240$, 0.217 and 0.249 (see chapter 7, for detail).

Competition in PDF

P model, Log-normal model, A&A model

Competition in PDFs of fluid particle accelerations (Gotoh and Bodenschatz)

A&A Model

log-normal Model

p Model

Competition II

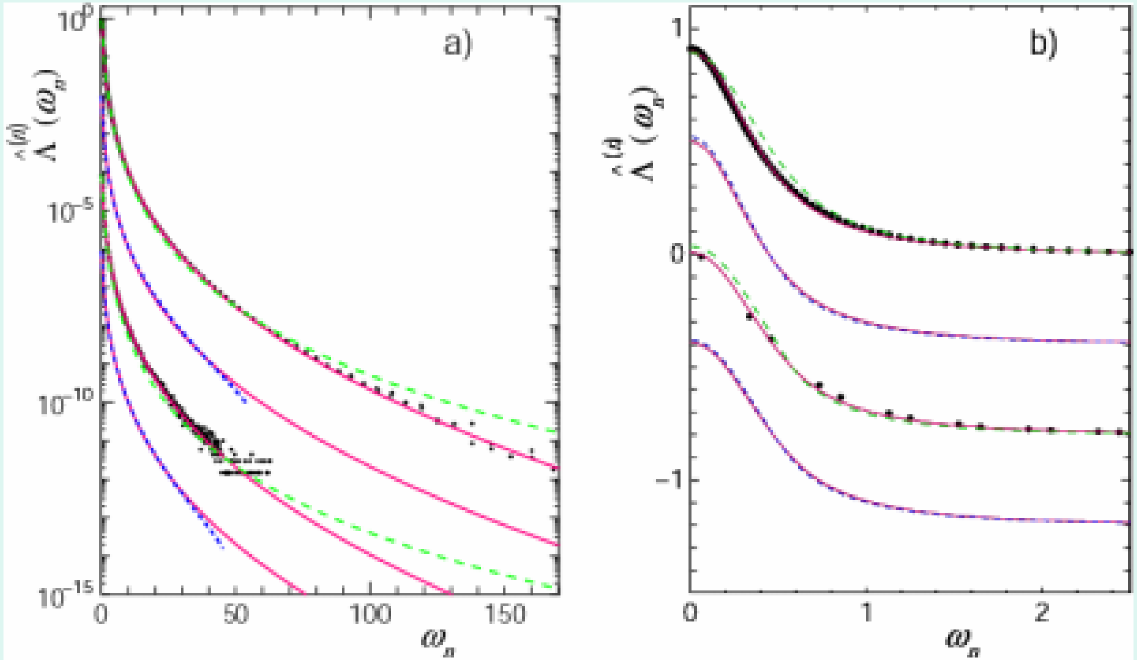

Fig. 6.6. Analyses of the PDF's of *fluid particle accelerations*, measured by Gotoh et al. at $R_\lambda = 380$ (circles in the top set) and by Bodenschatz et al. at $R_\lambda = 690$ (circled in the bottom set), by means of the PDF's $\hat{\Lambda}^{(n)}(\omega_n)$ by the harmonious representation (solid line) and by the log-normal model (dashed line) are plotted on (a) log and (b) linear scales. The PDF's by the p model (dotted line) are compared with the PDF's by the harmonious representation (solid line). Results are displayed in pairs. The solid lines in each set of pairs are the same. For better visibility, each PDF is shifted by −2 unit in (a) and by −0.4 in (b) along the vertical axis. Parameters are given in the text.

Competition II

Competition in PDFs of velocity fluctuations (Gotoh)

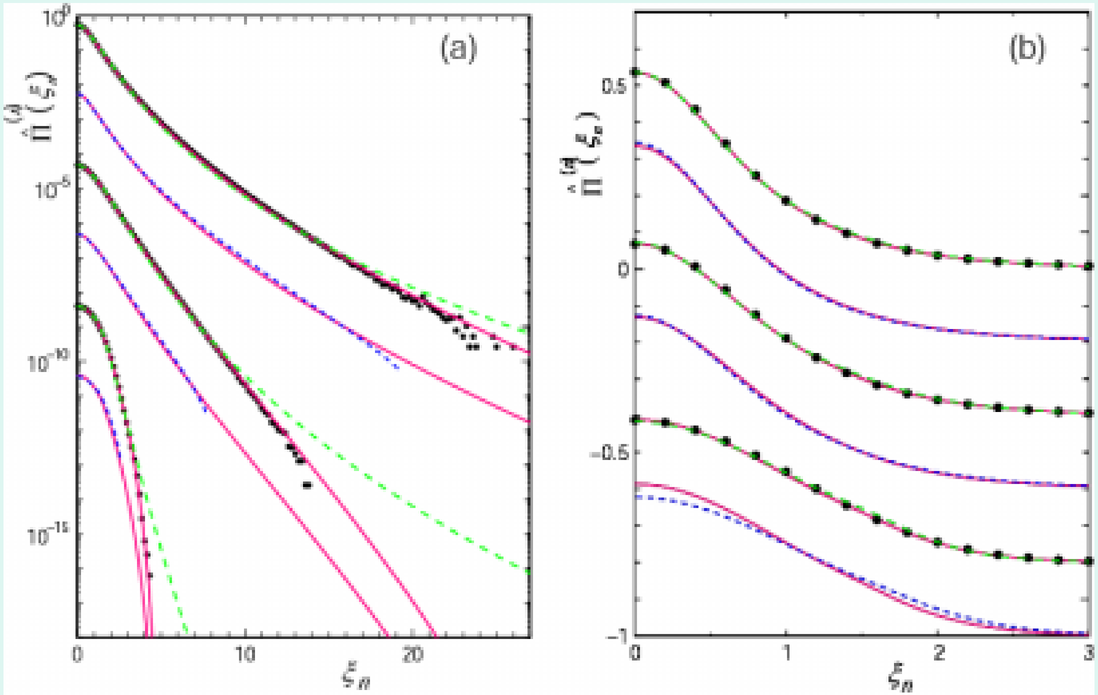

Fig. 6.5. Analyses of the PDF's of the velocity fluctuations (closed circles) for three different measuring distances, observed by Gotoh et al. at $R_\lambda = 380$, with the help of the PDF's $\hat{\Pi}^{(n)}(\xi_n)$ by the harmonious representation (solid line) and by the log-normal model (dashed line) are plotted on (a) log and (b) linear scales. The PDF's by the p model (dotted line) are compared with the PDF's by the harmonious representation (solid line). Comparisons are displayed in pairs. The solid lines in each set of pairs are the same. For better visibility, each PDF is shifted by -2 unit in (a) and by -0.2 in (b) along the vertical axis. Parameters are given in the text.

Superfluid Turbulence

J.Maurer and P.Tabeling

Europhys. Lett. 43 (1998) 29-34

Maurer & Tabeling

① DC motor
② blades
③ Pitot tube

$$p_{\text{meas}}(t) = p(t) + \rho_s U_s u_s(t) + \rho_n U_n u_n(t)\,,$$

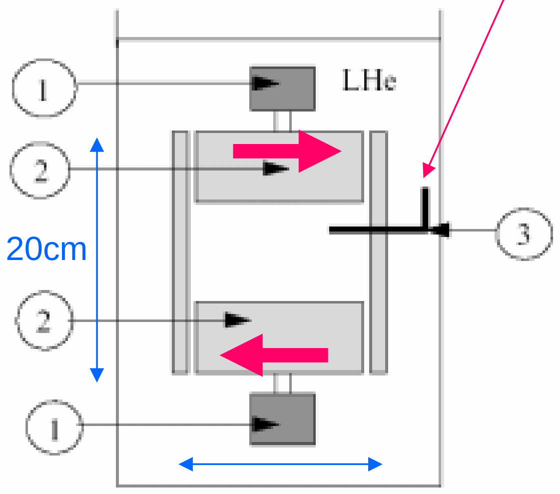

Fig. 1

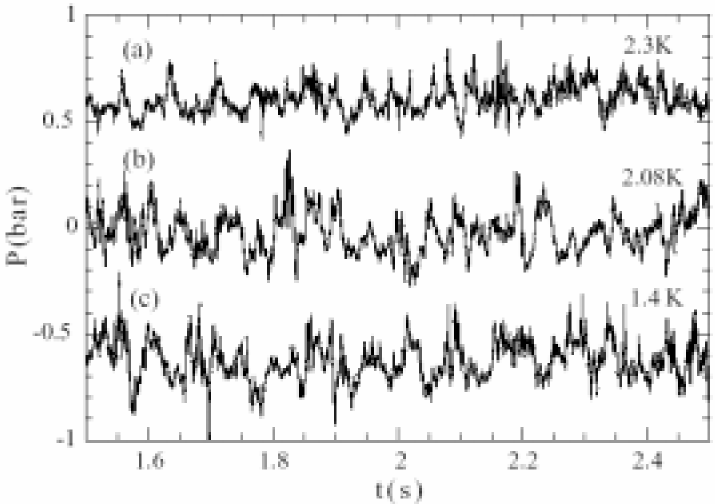

Fig. 2

Fig. 1. – Sketch of the experiment; 1: DC Motor, 2: propellor, 3: probe.

Fig. 2. – Time series obtained for a frequency rotation of 6 Hz, at three different temperatures: (a) 2.3 K (at a 1 bar pressure); (b) 2.08 K; (c) 1.4 K. The time series have been shifted vertically so as to make their representation clear.

Maurer & Tabeling

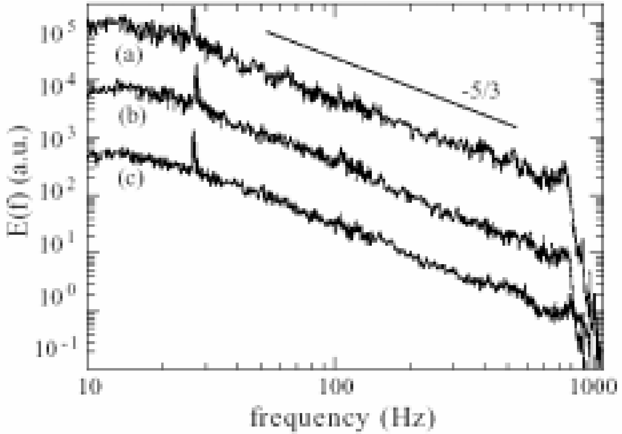

Fig. 3

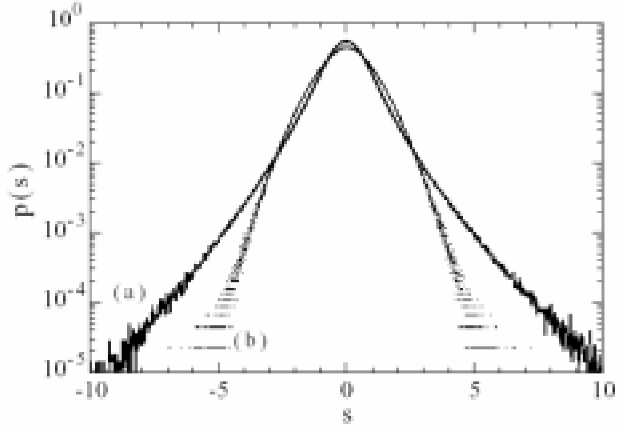

Fig. 4

Fig. 3. – Energy spectra obtained in the same conditions, but at different temperatures: (a) 2.3 K; (b) 2.08 K; (c) 1.4 K. The spectra have been shifted vertically so as to make their representation clear.

Fig. 4. – pdf of the velocity increments obtained for time separations equal to (a) $\delta t = 1$ ms (corresponding to the smallest scale we can resolve) and (b) $\delta t = 100$ ms (which is representative of a large scale), at $T = 1.4$ K; the abcissa s is rescaled so as the variances of the distributions are equal to one.

Maurer & Tabeling

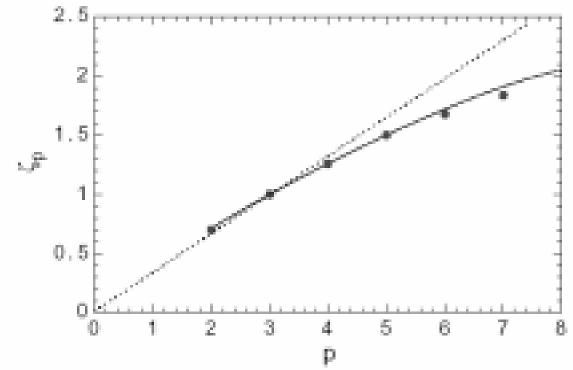

Fig. 5. – Exponents of the structure functions of the absolute values of the longitudinal velocity increments, up to $p = 7$, for $T = 1.4$ K (black disks); the full line represents the current values found in normal fluid turbulence; the dashed line is the Kolmogorov line.

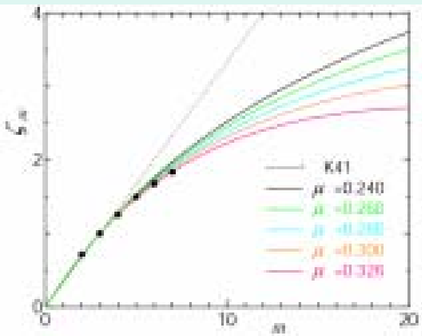

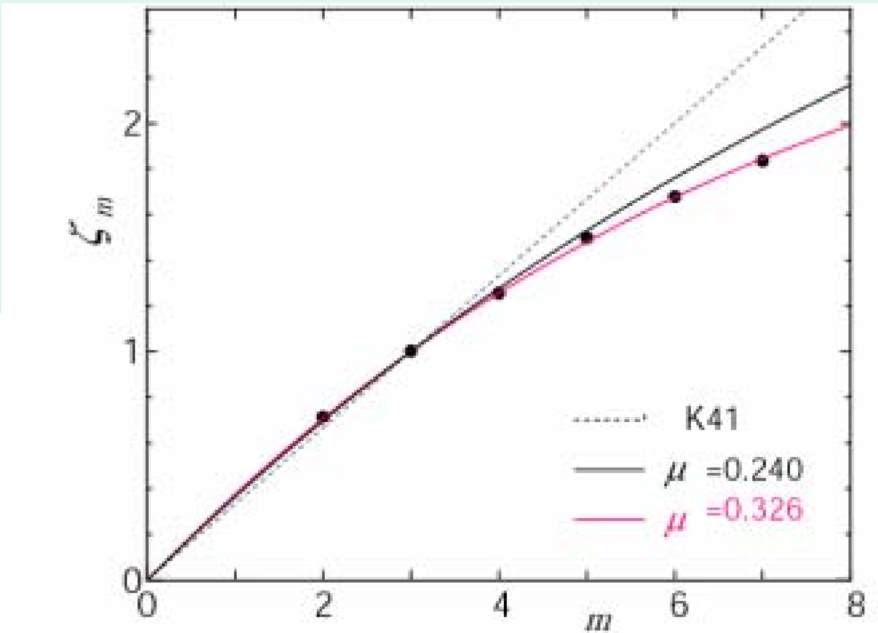

Maurer & Tabeling

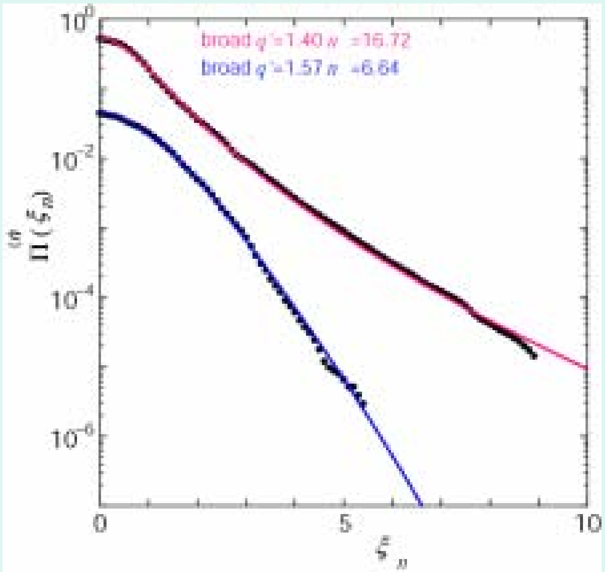

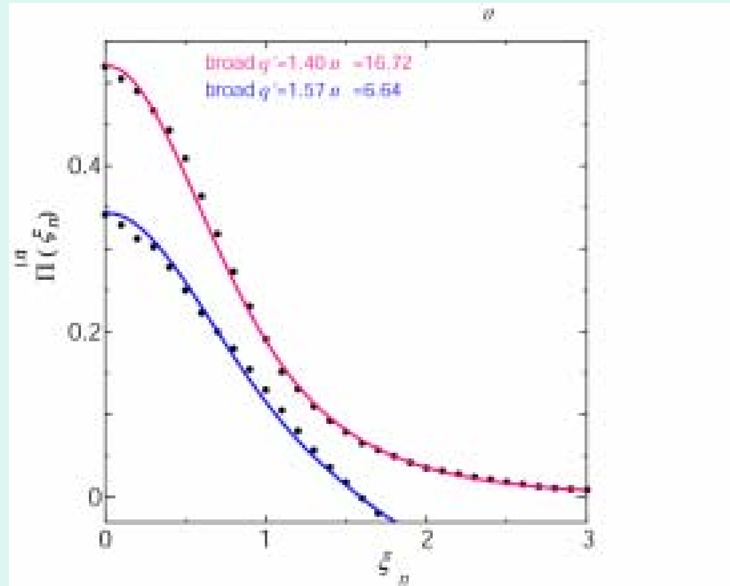

μ =0.326, α_0=0.388, X =1.18 (q =0.543)

Re ~ 2 x 10^6

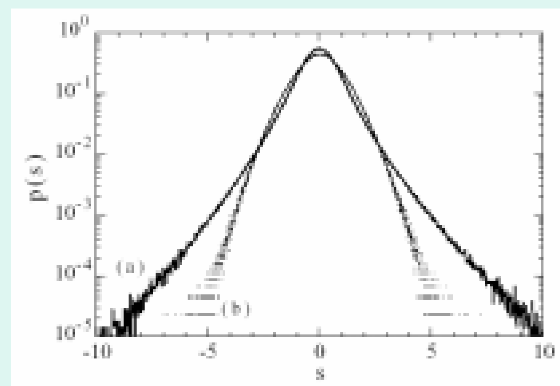

Conclusion and Prospects

Conclusion

- We showed that A&A model explains experimental and simulational PDFs quite accurately both in classical and quantum turbulences.
- So accurate, we expect that we can extract useful information for underlying dynamics of the systems from their analyses.
- Several future problems
  - Proof of the assumption of the multifractal distribution of singularities is in progress with the help of the data from the experiment in the wind tunnel and from DNS.
  - Search for a dynamical foundation of A&A model is in progress.

Vortex tangle in superfluid He

Prospects

- Since vorticity in superfluid is quantized, investigations of the vortex tangle in superfluid ^{4}He and ^{3}He are desirable in order to see what is the origin of the singularities and why their distribution is multi-fractal.
  - If the singularity originates from the core of vortex.
    → Multifractality of turbulence in normal fluid can be related to various values of vorticities in the fluid.
    → The vortex tangle may be uni-fractal.
    → Tangle does not exhibit intermittency.
  - If the singularity originates from the reconnection of vortices.
    → Multifractality of turbulence in normal fluid is related to the distribution of reconnection points in the fluid.
    → The vortex tangle may be also multi-fractal.
    → Tangle does exhibit intermittency.
- The analysis of simulations of vortex tangle conducted by Tsubota (Osaka City U) is highly desirable.

Thank you for your attention.